Hybrid Chaotic Scheme for Secure OFDM-PON Transmission

Huda Ismail Olewi
Department of Computer Engineering
Al-Nahrain University
Baghdad, Iraq
hudaalali33@gmail.com

Raad Sami Fyath
Department of Computer Engineering
Al-Nahrain University
Baghdad, Iraq
rsfyath@yahoo.com

***Abstract*—Different chaotic security schemes have been applied in the literature to secure transmission over orthogonal frequencies-division multiplexing (OFDM)-passive optical networks (PONs). All these schemes have been based on three-dimensional (3D) or four-dimensional (4D) chaos systems and have been applied to direct-detection (DD) OFDM-PONs. This paper proposes the use of 7D hybrid chaotic scheme to provide physical-layer security in both DD and coherent OFDM-PONs. The hybrid scheme uses a combination of 3D chaotic mapping scheme and 4D chaotic discrete Hartley transform precoding. The proposed chaotic security scheme is applied successfully for both DD-and coherent OFDM-PONs, and the results show that the security is very sensitive to initial conditions of both subchaotic systems.**

Keywords— Chaotic secure OFDM-PON; Optical orthogonal frequency-division multiplexing; Passive optical networks; Chaotic discrete Hartley transform precoding.

I. INTRODUCTION

Passive optical network (PON) supports cost-effective access network services and is characterized by efficient use of optical fiber resources to provide point-to-multipoint (i.e., multiusers) services [1]. The technology behind PON services is based on using power splitting without using in-line optical amplifiers (OA) [2]. A 1:N optical splitter plays as an interface between the optical line terminal (OLT) and N users. Each user is called optical network unit (ONU). The OLT is connected to the splitter through a feeder optical fiber while each splitter output is connected by a short drop fiber to provide services to one of the users , see Fig. 1. First generation of PONs uses intensity modulation (IM)/direct detection (DD) scheme to transmit up to 10 Gbps data over around 20 km transmission distance [3]. The IM/DD scheme offers low-cost implementation since the receiver does not use a local laser for the detection process . To support the rapidly traffic demand associated with emerging bandwidth-rich multimedia services such as internet of things (IoT) and 5G network, advanced PONs may incorporate different optical signal processing techniques Among thesee techniques are

i. Orthogonal frequency-division multiplexing (OFDM) which leads to DD-OFDM PON characterized by high spectral efficiency and robustness against fiber dispersion [4]. Further, OFDM reduces the level of equalization at the receiver end.
ii. Aggregation of transmissions service using multiplexing technique such as wavelength-divisionmultiplexing (WDM), time-division multiplexing (TDM), or both multiplexing techniques (TWDM) [5].

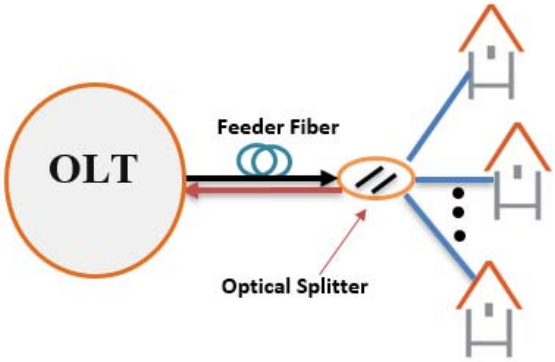

Fig. 1. Block diagram of PON.

iii. Coherent detection to increase the transmission data rate and distance [6]. The coherent PON receiver uses a local laser operating synchronously with the unmodulated transmitter laser and hence increasing the cost of the photoreceiver. However, coherent receiver offers many advantages such higher sensitivity compared with DD counterpart and its inherent wavelength selectivity. Tuning the local laser at the ONU enables the selection of the desired channel. Further, digital signal processing (DSP) can be used at the ONU to compensate the effect of fiber dispersion and nonlinearities . These features can also seen when the OFDM scheme is implemented under coherent-detection environment. This leads to high performance PON called coherent (CO)-OFDM PON.

The next generation (NG) PONs are expected to operate with data rate approaching 100 Gbps per channel wavelength and can support transmission distance beyond 100 km .

OFDM technique has become a promising solution to meet the increasing data traffic demand in next PONs . This is due to OFDM inherent advantages, namely high-spectral efficiency, high-antidispersion capability, and high tolerance to nonlinear fiber optics. However, OFDM-PON faces two main problems

i. The OLT transmits user data to all ONUs during downstream transmission. This data is vulnerable to eavesdropping by illegal users which would results in information leakage [7]. Encryption the data in media access control (MAC) layer does not encrypt the information in header. The illegal ONU can use the unencrypted header to decrypt the entire data . Thus,

encryption data at the physical layer is required in PONs during downstream transmission.

ii. OFDM is based on multisubcarrier modulation scheme and hence severs from relatively high peak-to-average power ratio (PAPR).

To solve these two problems, chaos-based physical-layer security schemes have been proposed for OFDM-PON by different research groups and some of the schemes have been supported by PAPR reduction techniques. The chaotic system is based on unpredictable nonlinear dynamics having very high sensitivity to initial conditions [8]. This increases the pseudo randomness and the size of the generated encryption key. Scanning the literature reveals that all the chaotic encryption schemes for OFDM-PON, except Ref. [13], are based on three-dimensional (3D) [9,10] and 4D chaos [11,12]. In Ref. [13], the authors used 7D chaotic security scheme for OFDM-PON. Further, to the authors opinion, all the chaotic security schemes have been applied only to DD-OFDM PONs. Further, some joint chaotic and PAPR reduction schemes with the chaotic sequence have been introduced to OFDM-PON.

The aim of this paper is to introduce virtual 7D chaotic security scheme which can be applied for both direct detection and coherent OFDM-PONs. The scheme uses a hybrid of two uncoupled chaotic security subsystems (CSSs) of degrees 3 and 4. This enables the proposed security scheme to control chaotically seven parameters of the OFDM physical layer. According to that, the hybrid chaotic security scheme (HCSS) will have higher security level and larger key space compared with the used CSSs. Further, the features of each of the CSS are reserved in the hybrid scheme.

II. Concepts of the Proposed 7D Hybrid Chaotic Scheme

Figs. 2 and 3 show block diagrams for the investigated chaotic secure OFDM-PONs operating under direct detection and coherent detection, respectively. A 7D hybrid chaotic scheme (HCS) is used to control seven parameters of the OFDM physical layer and hence ensures high-level security operation of the PON. The HCS-based OFDM uses two subchaotic secure schemes based on 3D and 4D chaotic systems, see Fig. 4. In this work, the HCS uses 3D chaotic constellation mapping scheme and 4D chaotic discrete Hartley transform-based scheme to secure the transmission of both DD-and CO-OFDM PON.

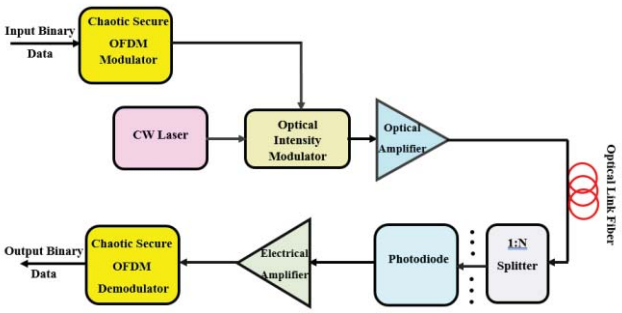

Fig. 2. Block diagram of secured direct detection OFDM-PON.

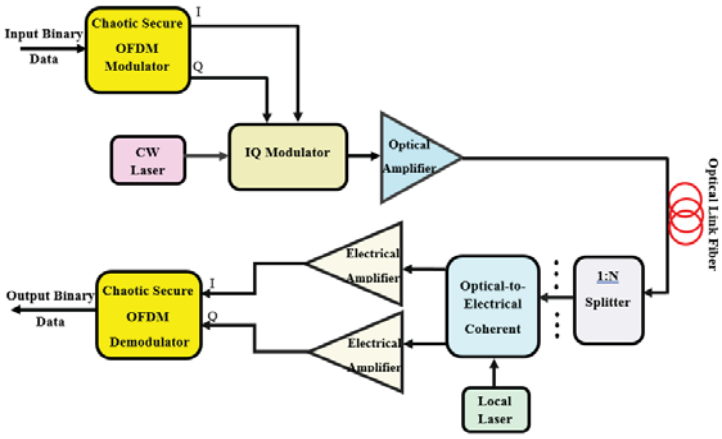

Fig. 3. Block diagram of secured coherent detection OFDM-PON.

Brief description of these two subchaotic schemes is given in the following

a) *3D Subchaotic Secure Scheme*

Chaotic constellation mapping scheme is used here to produce chaotic shifting of the quadrature phase-shift keying (QPSK) constellation to enhance the physical-layer security during OFDM transmission. The scheme uses 3D chaos based on three independent chaotic sequences ($x_1, x_2, and\ x_3$). The sequence x_1 is first converted to a binary sequence and then XORed with the input binary data. The other two chaotic sequences $x_2\ and\ x_3$ are used to produce dynamically chaotic shifting for the in-phase (I) and quadrature (Q) constellation components, respectively, of each transmitted QPSK symbol.

The 3D chaotic system used here is described by [10]

$$\begin{aligned} \dot{x_1} &= a_1(x_2 - x_1) + x_2x_3 \\ \dot{x_2} &= a_3x_1 - x_1x_3 - x_2 \\ \dot{x_3} &= x_1x_2 - a_2x_3 \end{aligned} \quad (1)$$

where the parameters a_1, a_2, and a_3 are real constants.

b) *4D Subchaotic Secure Scheme*

A 4D chaotic discrete Hartley transform (DHT) precoding scheme is adopted here to add additional level of security to the PON. This scheme also effectively reduces the PAPR of OFDM signals due to use of DHT precoding [12]. The key roles played by the used four chaotic sequences ($y_1, y_2, y_3,$ and y_4) can be briefly described as follows. y_1 and y_2 control the row and column permutations of the DHT matrix, respectively, and therefore yielding a chaotic DHT matrix. The other two chaotic sequences y_3 and y_4 are used to control subcarrier allocation and training sequence, respectively.

The chaotic sequences are generated using the following 4D chaotic system

$$\begin{aligned} \dot{y_1} &= b_1(-y_1 + y_2) + y_2y_3y_4 \\ \dot{y_2} &= b_2(y_1 + y_2) - y_1y_3y_4 \\ \dot{y_3} &= b_3y_2 - y_4 + b_4y_1y_2y_4 \\ \dot{y_4} &= -b_5y_4 + y_1y_2y_3 \end{aligned} \quad (2)$$

where the parameters $b_1,\ b_2,\ b_3,\ b_4, and\ b_5$ are real constants.

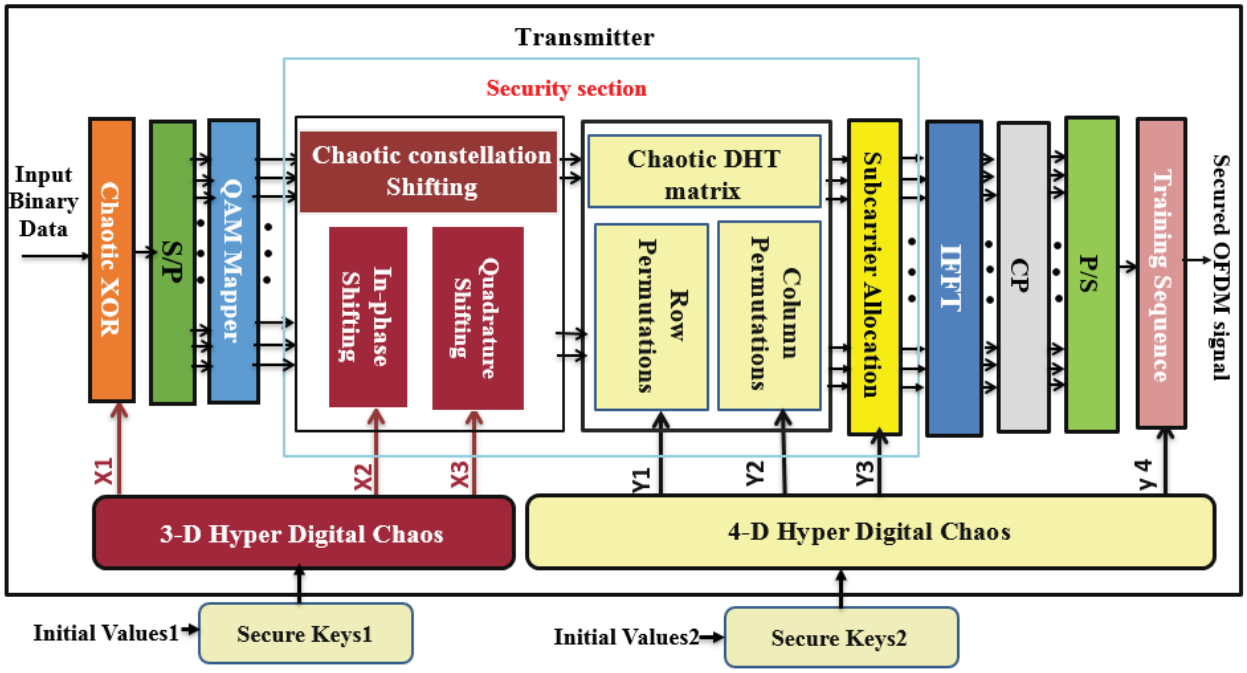

Fig. 4a. Block diagram of chaotic secure OFDM modulator.

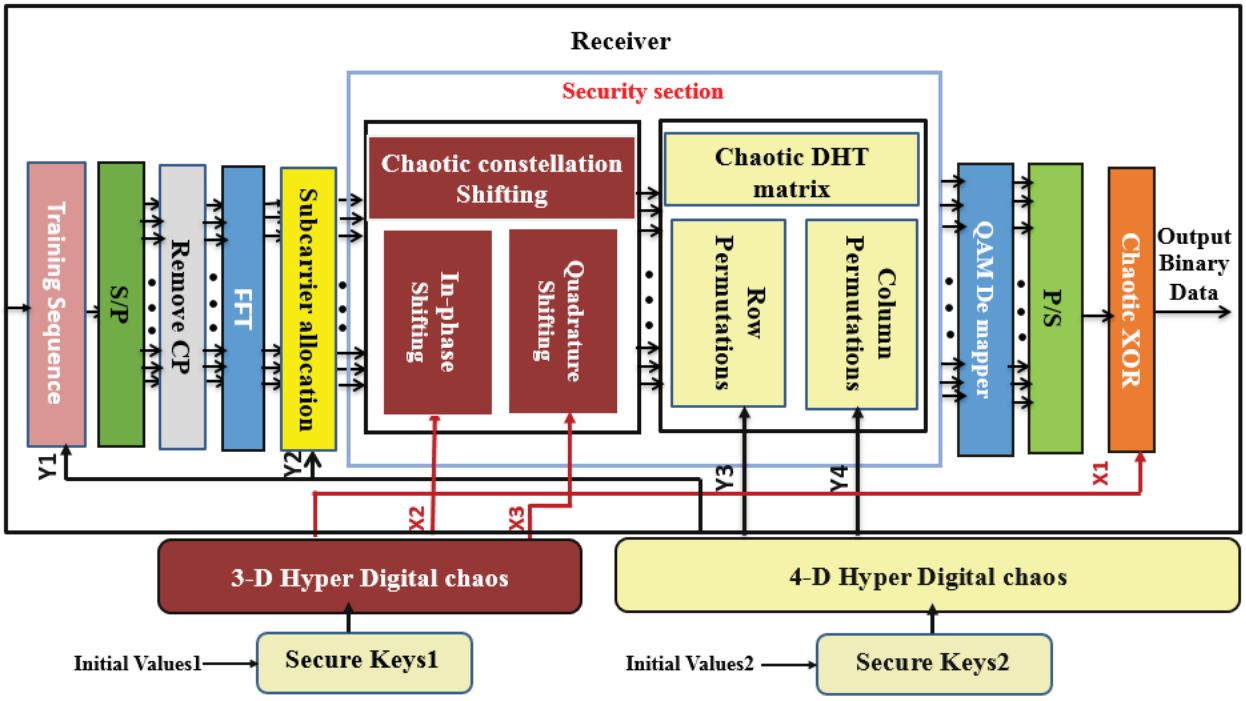

Fig. 4b. Block diagram of chaotic secure OFDM demodulator.

III. Simulation Results

The characteristics of the 3D chaotic system is illustrated in Fig. 5 assuming $a_1 = 10.0$, $a_2 = 8/3$, and $a_3 = 28$. The used initial conditions are $x_1(0) = 0.1$, $x_2(0) = 0.1$, and $x_3(0) = 0.1$. Parts a-c of this figure show the behavior of the 3D chaotic attractor. Parts d-f of the figure illustrate the normalize autocorrelation R_{x1x1} and crosscorrelations R_{x1x2} and R_{x1x3},respectively. The chaotic characteristics of the 4D system is given in Fig. 6 and obtained using $b_1 = 35, b_2 = 10$, $b_3 = 80, b_4 = 0.5$, *and* $b_5 = 10$. The used initial conditions are $y_1(0) = 1, y_2(0) = 1, y_3(0) = 1,$ and $y_4(0) = 1$. Investigating the results in Figures (5) and (6) reveal that both chaotic systems have excellent autocorrelation and crosscorrelation properties.

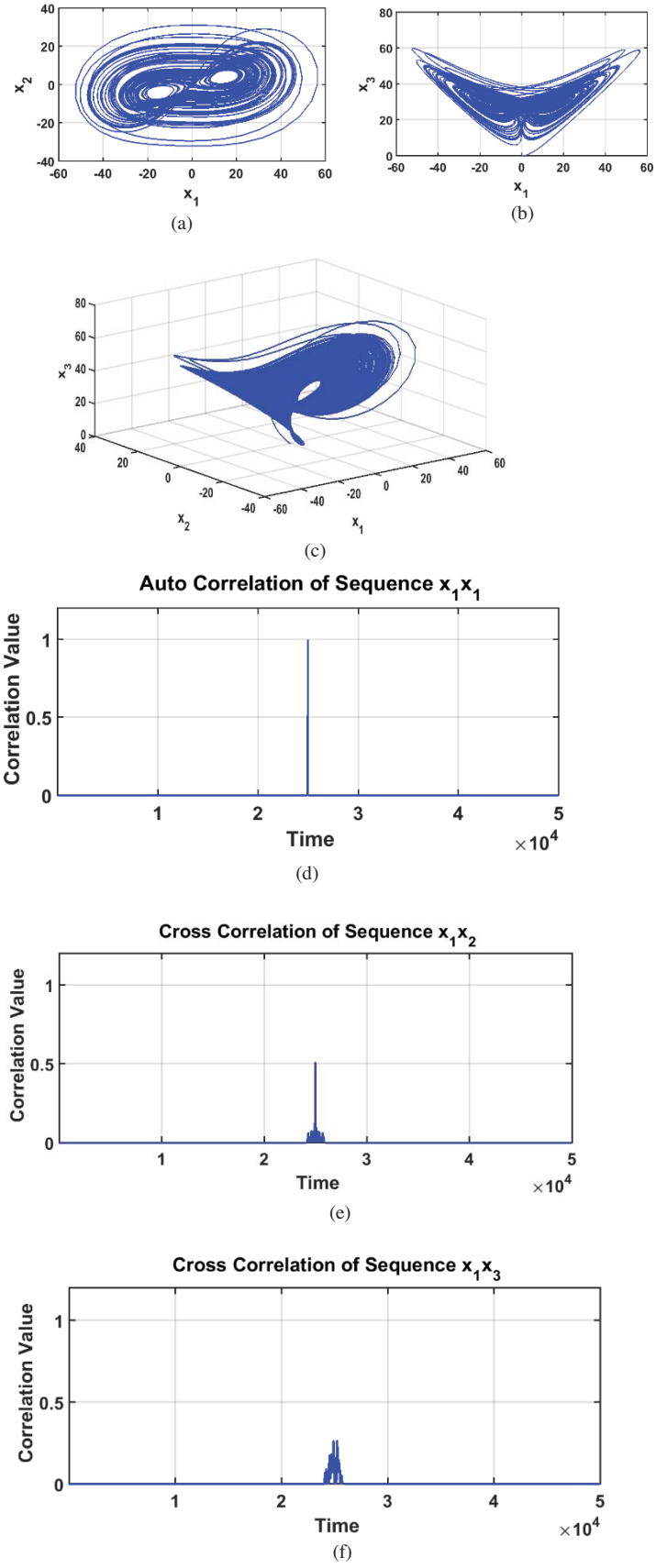

Fig. 5. Phase projections of the 3D hyperchaotic attractor (a) x_1-x_2 space projection (b) x_1-x_3 space projection (c) x_1-x_2-x_3 space projection (d) Autocorrelation R_{x1x1} (e) Crosscorrelation R_{x1x2} (f) Crosscorrelation R_{x1x3}.

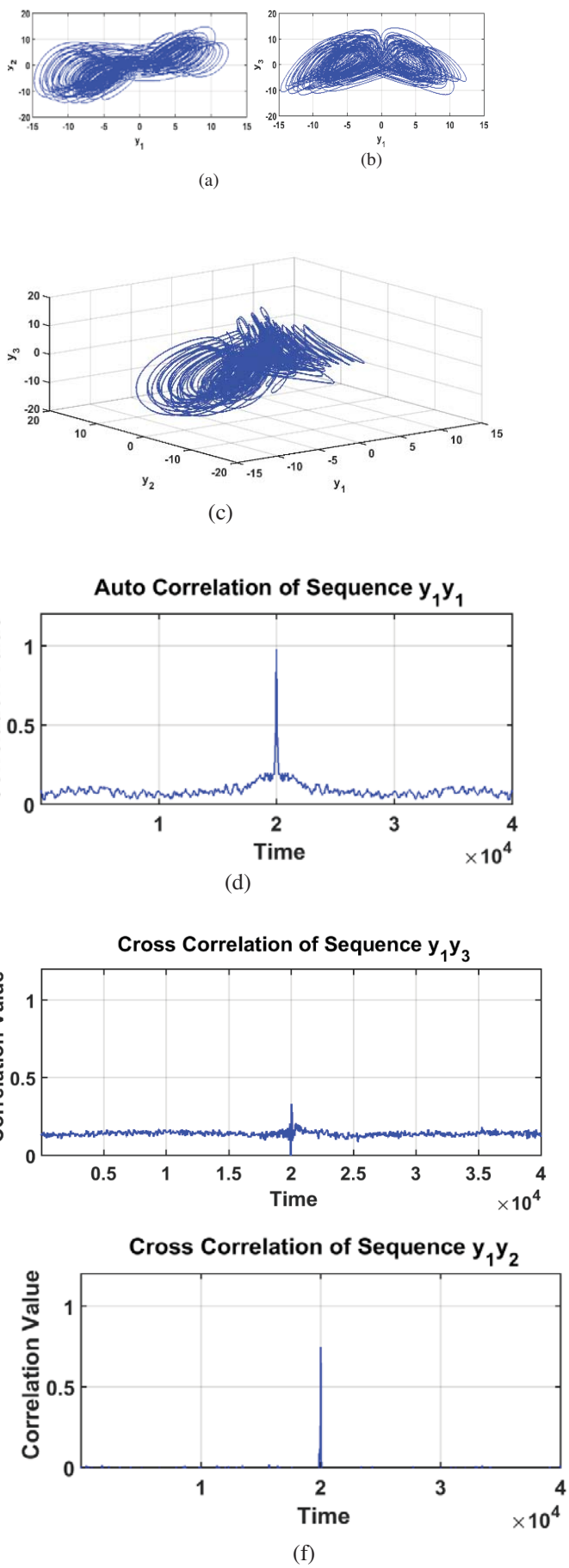

Fig. 6. Phase projections of the 4D hyperchaotic attractor (a) y_1-y_2 space projection (b) y_1 - y_3 space projection (c) y_1 - y_2 - y_3 space projection (d) Autocorrelation R_{y1y1} (e) Crosscorrelation R_{y1y2} (f) Crosscorrelation R_{y1y3}.

The 7D chaotic secure OFDM modulator and demodulator are built in Matlab environment and used as library elements in the commercial software "Optisystem version 15". The parameters used in the simulation are laser wavelength = 1550 nm, FFT size = 256, number of OFDM subcarriers = 128, and modulation format is QPSK.

The first simulation task is to address the transmission performance of 10 Gbps QPSK DD-OFDM PON over 40 km single-mode fiber. The system uses 5 GHz RF subcarrier to carry the input data before modulating the optical carrier. Fig. 7 shows the spectrum of the signals of different points of the system. The results in this figure highlights the fact that inserting the 7D chaotic scheme does not affect the operation principles of the DD-OFDM PON. Fig. 8a depicts the receiver constellation diagram when the chaotic demodulation uses the same initial conditions of the transmitter 7D chaotic system. The receiver BER $= 5.4 \times 10^{-4}$ in this case. Changing the initial condition of x_1 by 10^{-15} at the chaotic demodulator destroys the receiver constellation diagram (see Fig. 8b) and leading to a BER = 0.5.

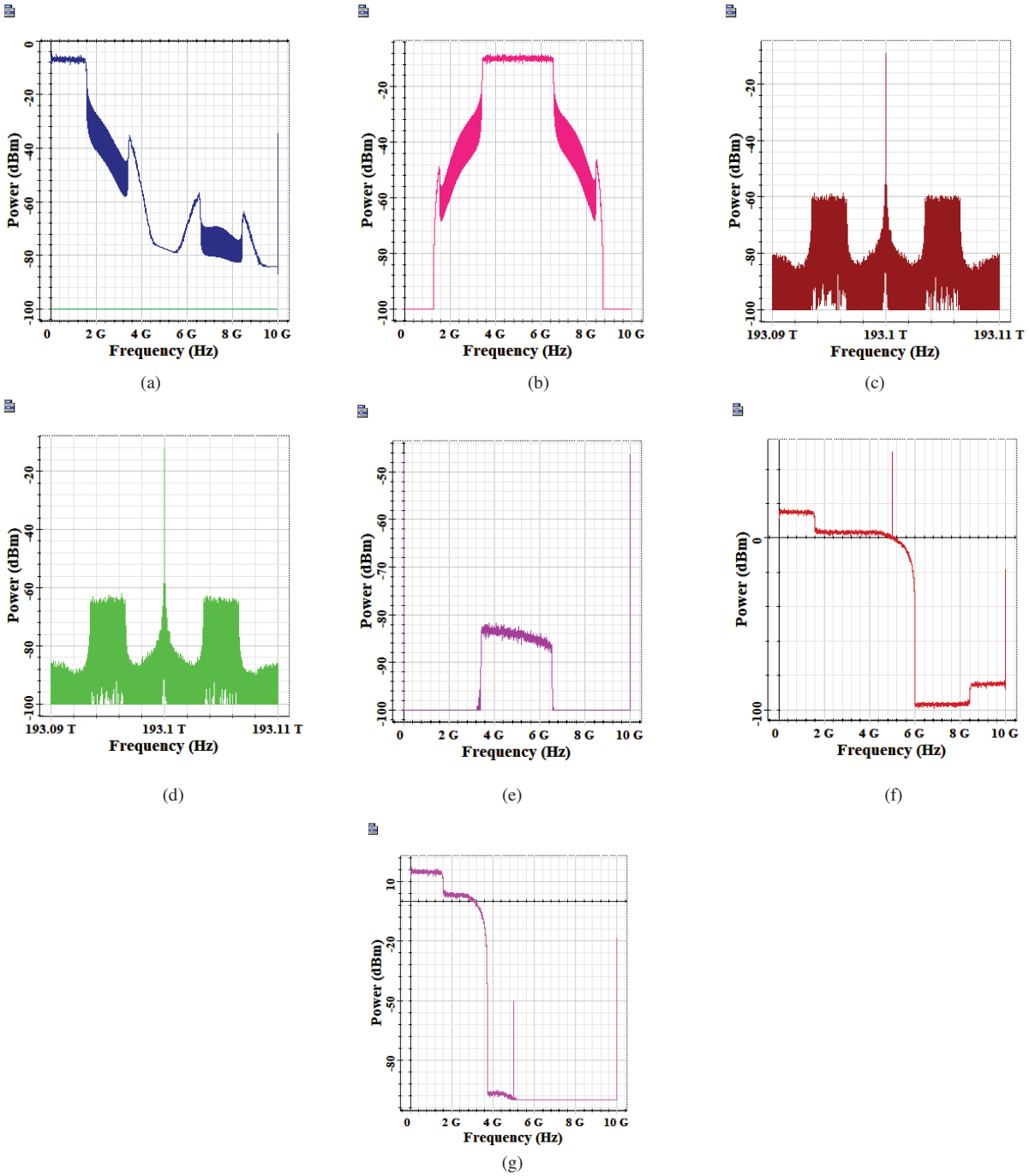

Fig. 7. Spectra of the signals at different points of 40 km DD- OFDM PON using 10 Gbps QPSK signaling with 0 dBm launch power (a) RF-spectrum after OFDM modulator (b) RF-spectrum after quadrature (c) Optical-spectrum after MZI modulator (d) Optical-spectrum after gaussian optical filter (e) RF-spectrum after photodiode (f) RF-spectrum after quadrature demodulator (g) RF-spectrum after receiver LPF.

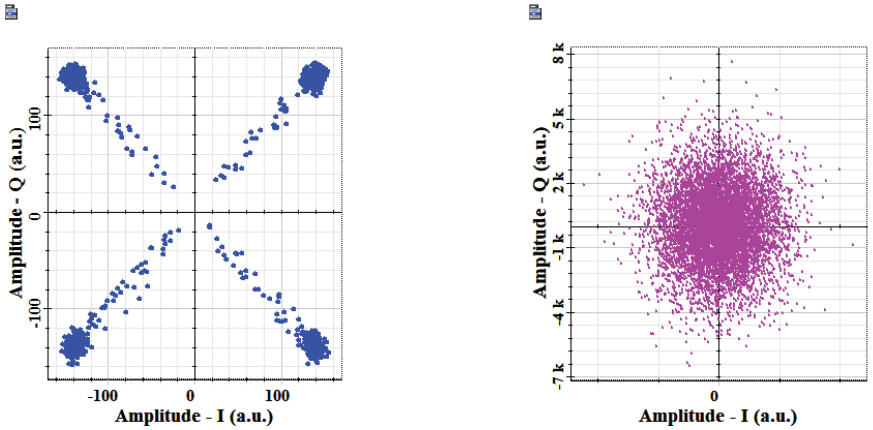

(a) (b)

Fig. 8 Receiver constellation diagram DD-OFDM PON operating with 10 Gbps signaling (a) Both transmitter and receiver chaotic scheme use the same initial values (b) One of the initial conditions, x_1 is increased by 10^{-15} at the receiver side.

The simulation is repeated for a coherent OFDM-PON operating with 10 km and 40 Gbps QPSK signaling. The receiver constellation diagram are given in Figs. 9a and 9b when the same initial conditions are used in both transmitter and receiver and one of the receiver initial conditions changes by 10^{-15}, respectively. The results again demonstrate the high sensitivity of the security of the system to initial conditions of the used chaotic system.

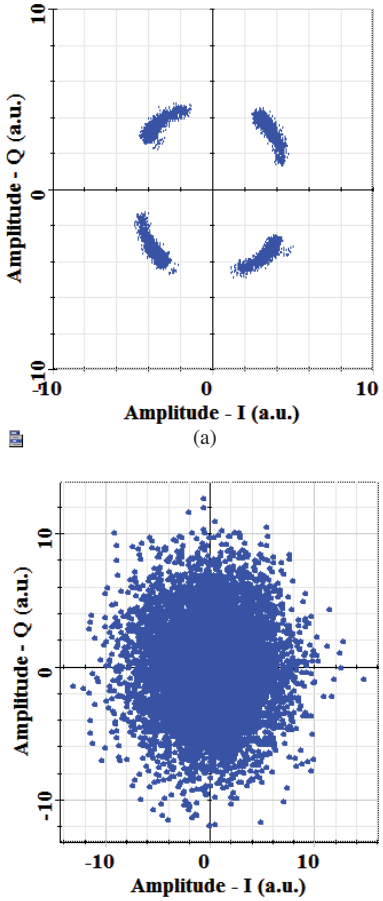

(a)

(b)

Fig. 9. Receiver constellation diagrams of the coherent OFDM-PON (a) Same initial values (b) One of the initial conditions is changed by 10^{-15} at the receiver side.

IV. Conclusion

A 7D chaotic security scheme has been proposed for OFDM-PONs. The scheme is based on a hybrid combination of two uncoupled 3D and 4D chaotic schemes. The main conclusions drawn from this study are any 3D and 4D chaotic security schemes can be used to construct the hybrid scheme and therefore, their security features are kept. Further, the proposed scheme can be applied for both direct-detection and coherent OFDM-PONs since it controls the parameters of the physical layer common between them. The security key space increases when compared with that related to the used subchaotic schemes.

The work can be extended in the future to incorporate different pairs of subchaotic systems. Further, one can go to use chaose with degree more than 7 to increase the physical-layer security level of OFDM-PONs.

References

[1] Y. Nakayama and D. Hisano, IEEE Transactions on Communications, vol. 67, no. 11, pp. 7642-7655, Nov. 2019.
[2] J. A. Altabas, G. S. Valdecasa, L. F. Suhr, M., Journal of Lightwave Technology, vol. 37, no. 2, pp. 651-656, Jan. 2019.
[3] Y. Li, J. Han, and X. Zhao, IEEE Access, vol. 7, pp. 43137-43142, Apr. 2019.
[4] J. Peng , Y. Sun, H. Chen, T. Xu , Z. Li, Q. Zhang , and J. Zhang, IEEE Photonics Journal, vol. 11, no. 1, Article no. 7201514, pp. 1-14, Feb. 2019.
[5] L. B. Du, X. Zhao, S. Yin, T. Zhang, A. E. T. Barratt, J. Jiang, D. Wang, J. Geng, C. DeSanti, and C. F. Lam, IEEE Journal of Lightwave Technology, vol. 37, no. 3, pp. 688-697, Feb. 2019.
[6] F. Pittalà, I. N. Cano, C. Bluemm, M. Schaedler, S. Calabrò, G. Goeger, R. Brenot, C. Xie, C. Shi, G. N. Liu, G. Charlet, and M. Kuschnerov, IEEE Photonics Technology Letters, vol. 31, no. 15, pp. 1229-1232, Aug. 2019.
[7] M. Bi, X. Zhuo, G. Yang, M. Hu, B. Fan, X. Yang, W. Hu, Optical Fiber Technology, vol. 51, pp. 64-70, May 2019.
[8] S. Li , M. Cheng, L. Deng, S. Fu, M. Zhang, M. Tang, P. Shum, and D. Liu, Journal of Lightwave Technology, vol. 36, no. 20, pp. 4826–4833, Oct. 2018.
[9] S. Vaidyanathan, O. A. Abba, G. Betchewe, and M. Alidou, International Journal of Automation and Control, vol. 13, no. 1, pp. 101–121, Jan. 2019.
[10] A. Sultan, X. Yang, A. A. E. Hajomer, and W. Hu, IEEE Photonics Technology Letters, vol. 30, no. 4, pp. 339–342, Feb. 2018.
[11] J. Zhong, X. Yang, and W. Hu, IEEE Photonics Technology Letters, vol. 29, no. 12, pp. 991–994, June 2017.
[12] A. A. E. Hajomer, X. Yang, and W. Hu, IEEE Photonics Journal, vol. 10, no. 2, Feb. 2018.
[13] Z. Hu and C. K. Chan, Journal of Lightwave Technology, vol. 36, no. 16, pp. 3373–3381, Aug. 2018.